Bounds on heat transport in Bénard-Marangoni convection

George Hagstrom
Department of Physics, The University of Texas at Austin, Austin, Texas 78712, USA

Charles R. Doering*
Department of Mathematics, Department of Physics, Michigan Center for Theoretical Physics, and Center for the Study of Complex Systems, University of Michigan, Ann Arbor, Michigan 48109-1043, USA
(Received 19 December 2009; published 5 April 2010)

For Pearson's model of Bénard-Marangoni convection, the Nusselt number Nu is proven to be bounded as a function Marangoni number Ma according to $\mathrm{Nu} \leq 0.838 \times \mathrm{Ma}^{2/7}$ for infinite Prandtl number and according to $\mathrm{Nu} \lesssim \mathrm{Ma}^{1/2}$ uniformly for finite Prandtl number. The analysis is also used to raise the lower bound for the critical Marangoni number for energy stability of the conduction solution from 56.77 to 58.36 when the Prandtl number is infinite.

DOI: 10.1103/PhysRevE.81.047301 PACS number(s): 47.55.pf, 47.27.te, 47.10.A−

Rayleigh-Bénard convection, the buoyancy-driven flow in a layer of fluid heated from below and cooled from above, is a paradigm for complex nonlinear dynamics, pattern formation, and turbulent transport. Heat transport properties of convective flow are of primary interest in many applications and the dependence of the enhanced effective thermal conductivity (the Nusselt number Nu) on the basic system parameters has been the subject of much theoretical, mathematical, computational, and experimental research [1–5]. The dynamics and heat transport properties of surface-tension-driven Bénard-Marangoni convection has been studied much less despite its importance for many applications [6–8]. In this Brief Report, we derive heat transport bounds for Pearson's [6] model of Bénard-Marangoni convection. This model has recently been the subject of high-Marangoni direct numerical simulations [9,10] and this work provides a rigorous theoretical analysis of its fully nonlinear transport properties. The "background method" [2,11] is adapted to derive an upper bound on the Nusselt number as a function of the Marangoni number Ma and, as a side product, improve the energy stability bound for the conduction state in the infinite Prandtl number case. Here we present an application of the background method to a stress-driven flow [12] with boundary-condition coupling of the dynamical fields.

The basic model is

$$\mathrm{Pr}^{-1}\left(\frac{\partial \mathbf{u}}{\partial t} + \mathbf{u} \cdot \nabla \mathbf{u}\right) = -\nabla p + \Delta \mathbf{u}, \tag{1}$$

$$\nabla \cdot \mathbf{u} = 0, \tag{2}$$

$$\frac{\partial T}{\partial t} + \mathbf{u} \cdot \nabla T = \Delta T, \tag{3}$$

where $\mathbf{u}(\mathbf{x},t) = \mathbf{i}u(\mathbf{x},t) + \mathbf{k}w(\mathbf{x},t)$ is the velocity vector field, $p(\mathbf{x},t)$ is the pressure field, and $T(\mathbf{x},t)$ is the temperature field in a fluid layer of unit depth in the z direction ($0 \leq z \leq 1$). The bottom of the layer has no-slip, isothermal boundary conditions,

$$u|_{z=0} = 0 = w|_{z=0}, \quad T|_{z=0} = 0, \tag{4}$$

and the temperature and flow fields are coupled through the boundary conditions on the nondeformable, fixed-flux top surface

$$w|_{z=1} = 0, \quad \left.\frac{\partial T}{\partial z}\right|_{z=1} = -1, \tag{5}$$

$$\left[\frac{\partial u}{\partial z} + \mathrm{Ma}\frac{\partial T}{\partial x}\right]_{z=1} = 0. \tag{6}$$

All dynamical variables are periodic in the horizontal (x) direction. The length unit is the layer thickness h, the time unit is h^2/κ, and the temperature unit is qh/λ, where κ is the fluid's thermal diffusion coefficient, λ is its heat conductivity, and q is the imposed heat flux through the layer. The Prandtl number is $\mathrm{Pr} = \nu/\kappa$, where ν is the fluid's viscosity, and the Marangoni number is $\mathrm{Ma} = \gamma q h^2/\lambda\rho\nu\kappa$, where γ is the (negative of the) derivative of the surface tension with respect to temperature and ρ is the fluid density. The problem and results are described in two spatial dimensions but may be generalized to three dimensions by including a $\mathbf{j}v(\mathbf{x},t)$ y-velocity component satisfying $v|_{z=0}=0$ and $[\partial v/\partial z + \mathrm{Ma}\,\partial T/\partial y]_{z=1}=0$.

The heat flux is prescribed so enhancement of heat transport due to convection is indicated by a reduction of the temperature drop across the layer. Thus the Nusselt number is defined as $\mathrm{Nu} = -1/\bar{T}|_{z=1}$, where $\bar{T}|_{z=1}$ is the horizontally and time-averaged temperature at the top surface ($-1 \leq \bar{T}|_{z=1} < 0$).

In 1958, Pearson showed that the steady conduction solution, $\mathbf{u}=0$ and $T=-z$, is linearly unstable when the Marangoni number exceeds 79.61 [6]. In 1969, Davis showed that it is nonlinearly asymptotically stable for Marangoni numbers below 56.77 [7].

In the infinite Prandtl number case, the momentum Eq. (1) reduces to $\nabla p = \Delta \mathbf{u}$ so the incompressibility condition (2) implies that $\Delta p = 0$ and each component of $\mathbf{u}$ is biharmonic. In particular, $\Delta^2 w = 0$, so at each instant of time the Fourier transform in the x direction of the vertical component of the velocity $\hat{w}_k(z,t)$ satisfies

*doering@umich.edu

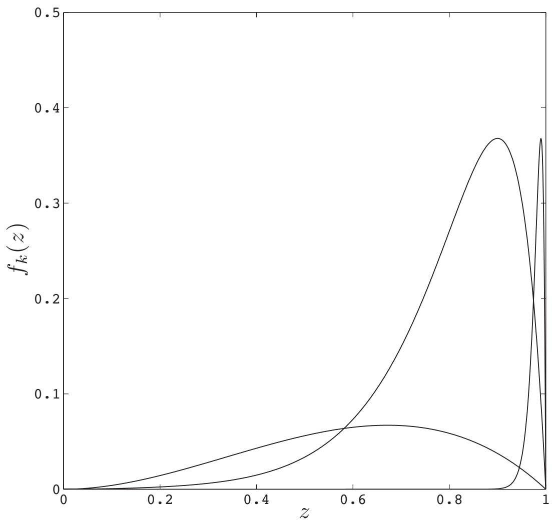

FIG. 1. Functions $f_k(z)$ for $k=1,10,100$.

$$\frac{d^4\hat{w}_k}{dz^4} - 2k^2\frac{d^2\hat{w}_k}{dz^2} + k^4\hat{w}_k = 0, \tag{7}$$

with boundary conditions

$$\hat{w}_k|_{z=0} = 0, \quad \frac{d\hat{w}_k}{dz}|_{z=0} = 0, \quad \hat{w}_k|_{z=1} = 0 \tag{8}$$

and

$$\frac{d^2\hat{w}_k}{dz^2}|_{z=1} = -k^2 \text{ Ma } \hat{T}_k(1,t). \tag{9}$$

This means that the vertical velocity is a linear (albeit nonlocal) functional of the temperature. The exact solution to Eqs. (7)–(9) is $\hat{w}_k(z,t) = -\text{Ma } \hat{T}_k(1,t) f_k(z)$, where

$$f_k(z) = \frac{k \sinh k}{2(\sinh k \cosh k - k)}\{kz \cosh(kz) - \sinh(kz) + [1 - k \coth(k)]z \sinh(kz)\}. \tag{10}$$

For large k, these non-negative functions are concentrated near $z=1$ while for small k, they are spread across the interval [see Fig. 1]. The modes $f_k(z) \to 0$ pointwise for $z \in (0,1)$ in both the $k\to\infty$ and $k \to 0$ limits.

The background method analysis begins by writing $T = \tau(z) + \theta(\mathbf{x},t)$, where $\tau(0)=0$ and $\tau'(1)=-1$. The profile function $\tau(z)$ is the "background" and the remainder $\theta(\mathbf{x},t)$ is the "fluctuation" satisfying

$$\frac{\partial\theta}{\partial t} + w\tau'(z) + \mathbf{u}\cdot\nabla\theta = \Delta\theta + \tau''(z), \tag{11}$$

with boundary conditions $\theta|_{z=0} = 0 = (\partial\theta/\partial z)|_{z=1}$. Multiplying Eq. (11) by θ and integrating over space,

$$\frac{1}{2}\frac{d}{dt}\int dx \int dz\theta^2 = -\int dx \int dz[|\nabla\theta|^2 + \tau'\theta w - \theta\tau'']. \tag{12}$$

To study the nonlinear energy stability of the conduction solution, choose $\tau(z) = -z$. Evidently, the conduction solution is absolutely stable when the quadratic form $Q\{\theta\} = \int[|\nabla\theta|^2 - w\theta]dxdz$ is positive definite; $Q\{\theta\}>0$ implies that $\int\theta^2 dxdz \to 0$ monotonically and exponentially as $t\to\infty$. In terms of the Fourier coefficients,

$$Q\{\theta\} = \sum_k \int_0^1 \left[\left|\frac{d\hat{\theta}_k}{dz}\right|^2 + k^2|\hat{\theta}_k|^2 - \text{Re}(\hat{\theta}_k\hat{w}_k^*)\right]dz. \tag{13}$$

The term with $k=0$ is manifestly non-negative so only $k \neq 0$, in which case $\hat{T}_k(1) = \hat{\theta}_k(1,t)$, need be considered. Then

$$\begin{aligned}\left|\int_0^1 \hat{\theta}_k\hat{w}_k^* dz\right| &\leq \text{Ma}|\hat{\theta}_k(1)|\int_0^1 |\hat{\theta}_k(z)| f_k(z) dz \\ &\leq \text{Ma}|\hat{\theta}_k(1)|\|\hat{\theta}_k\|\|f_k\| \leq \text{Ma}\left\|\frac{d\hat{\theta}_k}{dz}\right\|\|\hat{\theta}_k\|\|f_k\| \\ &\leq \frac{\text{Ma}\|f_k\|}{2|k|}\left(\left\|\frac{d\hat{\theta}_k}{dz}\right\|^2 + k^2\|\hat{\theta}_k\|^2\right),\end{aligned} \tag{14}$$

where $\|\cdot\|$ refers to the L_2 norm on [0,1]. In the above, the fundamental theorem of calculus and Cauchy-Schwarz inequality were utilized to show

$$|\hat{\theta}_k(1)| = \left|\int_0^1 \frac{d\hat{\theta}_k}{dz}dz\right| \leq \left\|\frac{d\hat{\theta}_k}{dz}\right\| \tag{15}$$

and the fact that $ab \leq (a^2+b^2)/2$ was used to separate the terms. If $\text{Ma}\|f_k\|/2|k| < 1$ for each $k\neq 0$, then Q will be a positive form. A sufficient condition for energy stability is thus

$$\text{Ma} < \sup_k \frac{2|k|}{\left(\int_0^1 f_k(z)^2 dz\right)^{1/2}} \tag{16}$$

and numerical evaluation shows that the critical value is at least 58.36. That is, Nu=1 for Ma<58.36.

Sustained convection is not impossible for higher values of the Marangoni number. The Nusselt number is defined by $\text{Nu} = -1/\bar{T}|_{z=1}$ but it may be expressed alternatively by multiplying the temperature evolution Eq. (3) by T and averaging over space and time to find

$$\frac{1}{\text{Nu}} = \langle|\nabla T|^2\rangle, \tag{17}$$

where $\langle\cdot\rangle$ denotes the space and time average. After averaging and an integration by parts, the fluctuation field's "energy" evolution equation (12) yields

$$0 = \langle|\nabla\theta|^2 + \tau'\theta w + \tau'\,\partial\theta/\partial z\rangle + \bar{\theta}|_{z=1}. \tag{18}$$

Combined with the identities

$$\bar{T}|_{z=1} = \tau(1) + \bar{\theta}|_{z=1} \tag{19}$$

and

$$\langle|\nabla T|^2\rangle = \langle|\nabla\theta|^2 + 2\tau'\,\partial\theta/\partial z + (\tau')^2\rangle, \tag{20}$$

this implies

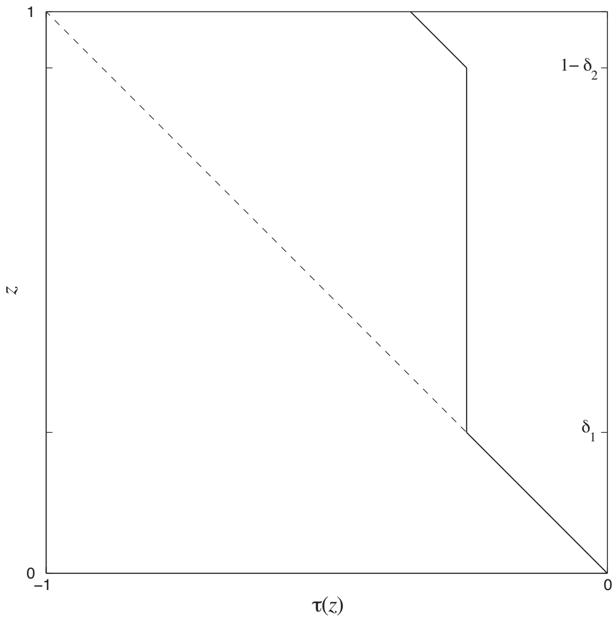

FIG. 2. Background profile $\tau(z)$ for Marangoni convection. The diagonal line is the conduction temperature profile.

$$\frac{1}{\mathrm{Nu}} = \langle |\nabla\theta|^2 + 2\tau' w\theta\rangle - 2\tau(1) - \int_0^1 \tau'(z)^2 dz. \qquad (21)$$

Thus, *if* the background profile $\tau(z)$ satisfying the boundary conditions can be chosen so that the quadratic functional $Q_\tau\{\theta\} = \int dx \int dz (|\nabla\theta|^2 + 2\tau' w\theta)$ is non-negative, *then* the Nusselt number is bounded above according to

$$\frac{1}{\mathrm{Nu}} \geq -2\tau(1) - \int_0^1 \tau'(z)^2 dz. \qquad (22)$$

The background profile may indeed be chosen appropriately. Fix the derivative of the background profile with $\tau'(z) = -1$ in layers of width δ_1 near the bottom boundary and δ_2 near the top boundary and $\tau(z) = \text{constant}$ in between as illustrated in Fig. 2. Explicitly,

$$\begin{aligned}\tau(z) &= -z \quad \text{for} \quad 0 < z < \delta_1 \\ &= -\delta_1 \quad \text{for} \quad \delta_1 < z < 1-\delta_2 \\ &= -\delta_1 - z + 1 - \delta_2 \quad \text{for} \quad 1-\delta_2 < z < 1. \end{aligned} \qquad (23)$$

Then $\mathrm{Nu} \leq 1/(\delta_1+\delta_2)$ as long as $Q_\tau\{\theta\}$ is positive for all θ satisfying the boundary conditions. In terms of the Fourier coefficients, this condition is that for each k,

$$\int_0^1 \left[\left| \frac{d\hat{\theta}_k}{dz} \right|^2 + k^2 |\hat{\theta}_k|^2 \right] dz + 2\int_0^{\delta_1} \mathrm{Re}(\hat{\theta}_k \hat{w}_k^*) dz + 2\int_{1-\delta_2}^1 \mathrm{Re}(\hat{\theta}_k \hat{w}_k^*) dz \geq 0. \qquad (24)$$

The analysis at the lower boundary proceeds as follows:

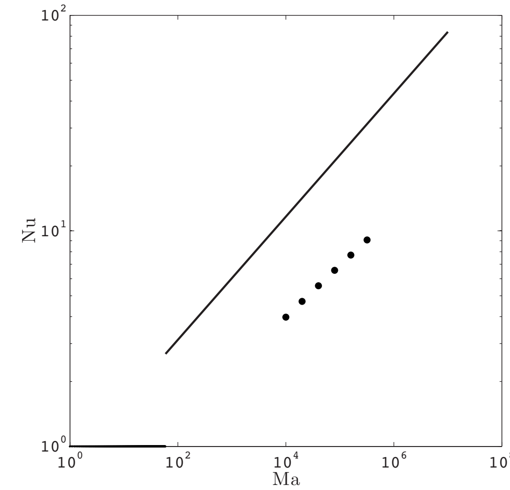

FIG. 3. Nusselt vs Marangoni number. Numerical data [9] are plotted together with the rigorous upper bounds.

$$\begin{aligned}\left| \int_0^{\delta_1} \hat{\theta}_k \hat{w}_k^* dz \right| &\leq \mathrm{Ma} |\hat{\theta}_k(1)| \int_0^{\delta_1} f_k(z) \left| \int_0^z \hat{\theta}_k'(\tilde{z}) d\tilde{z} \right| dz, \\ &\leq \mathrm{Ma} |\hat{\theta}_k(1)| \int_0^{\delta_1} f_k(z) \sqrt{z} \|\hat{\theta}_k'\| dz, \\ &\leq \mathrm{Ma} \left\| \frac{d\hat{\theta}_k}{dz} \right\|^2 \int_0^{\delta_1} \sqrt{z} |f_k(z)| dz, \end{aligned} \qquad (25)$$

where the fundamental theorem of calculus and Cauchy-Schwarz inequalities were used to bound $|\hat{\theta}_k(z)|$ and $|\hat{\theta}_k(1)|$ by $\sqrt{z}\|\hat{\theta}_k'\|$ and $\sqrt{1}\|\hat{\theta}_k'\|$, respectively.

Let $F(z) = \sup_k f(z)$. Each $f_k \sim z^2$ as $z \to 0$ so there is reason to believe that F might have the same behavior. In fact it does: $F(z) < cz^2$ for all $z \in [0,1]$ and the prefactor $c \approx 0.943$ is easily computed numerically. The upper boundary layer δ_2 may then be taken arbitrarily small, i.e., $\delta_2 \approx 0$, so there is no contribution from the upper boundary. Thus when $\delta_1 = (4c\,\mathrm{Ma}/7)^{-2/7}$, the quadratic form is non-negative and $\mathrm{Nu} < 0.838\,\mathrm{Ma}^{2/7}$.

Boeck and Thess [9] computed numerical solutions to the infinite Prandtl number problem over nearly 2 orders of magnitude in Ma, observing $\mathrm{Nu} \approx 0.446\,\mathrm{Ma}^{0.238}$ with a scaling exponent slightly less than $2/7 \approx 0.2857$. Their data are plotted with the bounds in Fig. 3.

Now consider the problem with finite Prandtl number. Employing the background decomposition, expression (21) for the Nusselt number still holds but in order to control w and incorporate the Marangoni condition it is necessary to utilize the full momentum equation. The space and time average of the dot product of Eq. (1) with $\mathbf{u}$ is, after integration by parts using the boundary condition,

$$0 = \langle |\nabla \mathbf{u}|^2 \rangle + \mathrm{Ma} \overline{\left(u \frac{\partial\theta}{\partial x} \right)}\Big|_{z=1} \qquad (26)$$

$$= \left\langle |\nabla \mathbf{u}|^2 + \mathrm{Ma} \frac{\partial}{\partial z} \left(u \frac{\partial\theta}{\partial x} \right) \right\rangle. \qquad (27)$$

Combining this with Eq. (21), we find

$$\frac{1}{\text{Nu}} = -2\bar{\tau}(1) - \langle \tau'^2 \rangle + \langle |\nabla\theta|^2 + 2\tau' w\theta \rangle + C\,\text{Ma}^{-2}\left\langle |\nabla \mathbf{u}|^2 + \text{Ma}\frac{\partial}{\partial z}\left(u\frac{\partial\theta}{\partial x}\right)\right\rangle, \qquad (28)$$

where C is an arbitrary constant chosen to be $C=1$.

The relevant quadratic form $\tilde{Q}_\tau\{\theta,\mathbf{u}\}$ is then

$$\tilde{Q}_\tau\{\theta,\mathbf{u}\} = \|\nabla\theta\|^2 + 2\int \tau' w\theta dxdz + \frac{1}{\text{Ma}^2}\|\nabla\mathbf{u}\|^2 + \frac{1}{\text{Ma}}\int \frac{\partial}{\partial z}\left(u\frac{\partial\theta}{\partial x}\right)dxdz, \qquad (29)$$

where from here on $\|\cdot\|$ denotes the L^2 norm on the two-dimensional domain. Again, the goal is to produce a background profile satisfying the boundary conditions and $\tilde{Q}_\tau \geq 0$ that minimizes $-2\bar{\tau}(1)-\langle\tau'^2\rangle$. Toward that end, choose $\tau(z)$ as in Eq. (23) so that the indefinite term $\sim\tau' w\theta$ reduces to the integral of the product of w and θ over regions of width δ_1 and δ_2 near the boundaries.

For the bottom layer, the fundamental theorem of calculus and Cauchy-Schwarz inequality imply

$$\left|\int dx\int_0^{\delta_1} dz\tau'\theta w\right| \leq \frac{\delta_1^2}{2}\left\|\frac{\partial\theta}{\partial z}\right\|\left\|\frac{\partial w}{\partial z}\right\| \leq \frac{1}{4}\left\|\frac{\partial\theta}{\partial z}\right\|^2 + \frac{\delta_1^4}{4}\left\|\frac{\partial w}{\partial z}\right\|^2. \qquad (30)$$

The upper layer analysis is different because θ is not zero on the upper boundary

$$\begin{aligned}\left|\int dx\int_{1-\delta_2}^{1} dz\tau'\theta w\right| &\leq \int dx\int_{1-\delta_2}^{1} dz|\theta|\left|\int_{1-z}^{1}\frac{\partial w}{\partial z}dz'\right| \\ &\leq \int dx\left[\int_0^1\left(\frac{\partial w}{\partial z'}\right)^2 dz'\right]^{1/2}\int_{1-\delta_2}^{1} dz|\theta|\sqrt{1-z} \\ &\leq \frac{\delta_2}{\sqrt{2}}\left\|\frac{\partial w}{\partial z}\right\|\|\theta\| \leq \frac{\delta_2}{\sqrt{2}\pi}\left\|\frac{\partial w}{\partial z}\right\|\left\|\frac{\partial\theta}{\partial z}\right\| \\ &\leq \frac{\delta_2}{2\sqrt{2}\pi}\left(\left\|\frac{\partial w}{\partial z}\right\|^2 + \left\|\frac{\partial\theta}{\partial z}\right\|^2\right), \end{aligned} \qquad (31)$$

where Poincaré's inequality, i.e., the fact that $\int_0^1 f(z)^2dz \leq \pi^{-2}\int_0^1 f'(z)^2dz$ when $f(0)=0=f(1)$, is used to bound $\|\theta\|$ in terms of $\|\frac{\partial\theta}{\partial z}\|$. The term from the boundary condition involving the Marangoni number must also be controlled by the L^2 norms of derivatives of $\mathbf{u}$ and θ,

$$\begin{aligned}\int \frac{\partial}{\partial z}\left(u\frac{\partial\theta}{\partial x}\right)dxdz &= \int\left(\frac{\partial u}{\partial z}\frac{\partial\theta}{\partial x} - \frac{\partial u}{\partial x}\frac{\partial\theta}{\partial z}\right) \\ &\leq \left(\left\|\frac{\partial u}{\partial z}\right\|\left\|\frac{\partial\theta}{\partial x}\right\| + \left\|\frac{\partial u}{\partial x}\right\|\left\|\frac{\partial\theta}{\partial z}\right\|\right) \\ &\leq \frac{1}{2\text{Ma}}\left(\left\|\frac{\partial u}{\partial z}\right\|^2 + \left\|\frac{\partial u}{\partial x}\right\|^2\right) + \frac{\text{Ma}}{2}\left(\left\|\frac{\partial\theta}{\partial x}\right\|^2 + \left\|\frac{\partial\theta}{\partial z}\right\|^2\right). \end{aligned} \qquad (32)$$

Inserting Eqs. (30)–(32) into Eq. (29),

$$\tilde{Q}_\tau \geq \frac{1}{2}\left\|\frac{\partial\theta}{\partial x}\right\|^2 - \frac{\delta_1^4}{2}\left\|\frac{\partial w}{\partial z}\right\|^2 - \frac{\delta_2}{2\sqrt{2}\pi}\left(\left\|\frac{\partial w}{\partial z}\right\|^2 + \left\|\frac{\partial\theta}{\partial z}\right\|^2\right) + \text{Ma}^{-2}\left(\frac{1}{2}\left\|\frac{\partial u}{\partial x}\right\|^2 + \frac{1}{2}\left\|\frac{\partial u}{\partial z}\right\|^2 + \left\|\frac{\partial w}{\partial x}\right\|^2 + \left\|\frac{\partial w}{\partial z}\right\|^2\right). \qquad (33)$$

The upper boundary layer thickness δ_2 may again be taken arbitrarily small without effecting the scaling. Therefore $\tilde{Q}_\tau$ is non-negative when $\delta_1 < 2^{1/4}\,\text{Ma}^{-1/2}$ which implies that $\text{Nu} \lesssim \text{Ma}^{1/2}$.

The $\text{Ma}^{1/2}$ bound is considerably looser than the infinite Prandtl number bound $\sim\text{Ma}^{2/7}$, although direct numerical simulations by Boeck and Thess [8,10] indicate that the heat transport scaling is not actually so much higher for the finite Prandtl number case. Not unexpectedly, the reason that the arbitrary-Pr bound is so much weaker is that the analysis is unable to take advantage of the strong relationship between the temperature and vertical velocity that is manifest in the infinite Prandtl number model. The situation is the same for analysis of Rayleigh-Bénard convection [2,3].

We thank T. Boeck, C.-C. Caulfield, R. R. Kerswell, W. Tang, and A. Thess for helpful discussions. This research was supported in part by NSF Award Nos. PHY-0555324 and PHY-0855335. Some of this work was performed at the GFD Program at Woods Hole Oceanographic Institution, supported by NSF and ONR, and some at the NSF's Institute for Mathematics and Its Applications at the University of Minnesota.

[1] L. N. Howard, J. Fluid Mech. **17**, 405 (1963).
[2] C. R. Doering and P. Constantin, Phys. Rev. E **53**, 5957 (1996).
[3] C. R. Doering, F. Otto, and M. G. Reznikoff, J. Fluid Mech. **560**, 229 (2006).
[4] H. Johnston and C. R. Doering, Phys. Rev. Lett. **102**, 064501 (2009).
[5] G. Ahlers, D. Lohse, and S. Grossmann, Rev. Mod. Phys. **81**, 503 (2009).
[6] J. R. A. Pearson, J. Fluid Mech. **4**, 489 (1958).
[7] S. H. Davis, J. Fluid Mech. **39**, 347 (1969).
[8] T. Boeck and A. Thess, Phys. Rev. Lett. **80**, 1216 (1998).
[9] T. Boeck and A. Thess, Phys. Rev. E **64**, 027303 (2001).
[10] T. Boeck, Adv. Space Res. **36**, 4 (2005).
[11] C. R. Doering and P. Constantin, Phys. Rev. Lett. **69**, 1648 (1992).
[12] W. Tang, C. Caulfield, and W. R. Young, J. Fluid Mech. **510**, 333 (2004).